

https://doi.org/10.1070/QEL16592

A GaInAs/AlInAs quantum cascade laser with an emission wavelength of 5.6 μm

I.I. Zasavitskii, N.Yu. Kovbasa, N.A. Raspopov, A.V. Lobintsov, Yu.V. Kurnyavko, P.V. Gorlachuk, A.B. Krysa, D.G. Revin

Abstract. **A quantum cascade laser based on a strain-compensated $Ga_{0.4}In_{0.6}As/Al_{0.58}In_{0.42}As$ heteropair is developed, which operates in the pulse regime in the wavelength range of 5.5–5.6 μm at temperatures of up to at least 350 K. It became possible due to an increase in the quantum well depth and to the usage of the two-phonon depopulation mechanism for the lower lasing level. The calculated voltage defect is about 100 meV. The laser epitaxial heterostructure was grown by the MOVPE method. It was investigated by the high-resolution X-ray diffraction technique. It is shown that the heterostructure has a high quality with bandwidths of main satellite peaks of 55 arcsec. The threshold current density is 1.6 kA cm^{-2} at 300 K. The characteristic temperature is T_0 = 161 K for the temperature interval of 200–350 K. For the laser of size 20 μm×3 mm with cleaved mirrors, the maximum pulsed power is 1.1 W at 80 K and 130 mW at 300 K.**

Keywords: *quantum cascade laser, GaInAs/AlInAs heteropair, MOVPE method, middle-IR spectrum range.*

1. Introduction

A quantum cascade laser (QCL) is a unipolar emission source based on interminiband electron transitions in a semiconductor nanoheterostructure [1, 2]. The QCL emission wavelength is defined by both the quantum well dimensions and the heteropair used. The latter determines the band offset, that is, the quantum well depth. Presently, by varying these two parameters and the material composition, QCLs are fabricated, which cover a wide IR emission spectral range of 3–250 μm. For operation in the actual middle-IR spectral range of 4–6 μm, a strain-compensated GaInAs/AlInAs heteropair is used, and the multilayer nanoheterostructure is grown, as a rule, by the molecular beam epitaxy method. The MOVPE (metal organic vapour phase epitaxy) method suggested in [3–5] possesses such advantages as a high rate of growth and the possibility of growing phosphorous-containing materials. However, a drawback of this method is the interface sharpness problem related to a higher growth temperature.

In the present work, a laser heterostructure based on a strain-compensated $Ga_{0.4}In_{0.6}As/Al_{0.58}In_{0.42}As$ heteropair was grown by the MOVPE method. A high quality of the structure is confirmed by X-ray diffraction spectra. The structure design corresponds to the emission wavelength of about 5.6 μm and utilises the two-phonon scheme for lower lasing level depopulation. In the pulsed regime, the operation temperature of the QCL reached 350 K and the radiation power exceeded 1.1 W at 80 K.

2. Laser heterostructure design and characterisation

It is well known that epitaxial growth of $Ga_{1-x}In_xAs$ and $Al_{1-y}In_yAs$ solid solutions on an InP substrate yields almost perfectly matched lattice constants at $x = 0.53$ and $y = 0.52$. In these compositions, the band offset in the conduction band is $\Delta E_c = 0.52$ eV. Such a value of the quantum well depth in the heterostructure considered is not sufficient for creating efficient lasers with the emission wavelength shorter than 6 μm, especially QCLs with the two-phonon depopulation mechanism for the lower lasing level. Hence, for increasing the quantum well depth, a heteropair is used, whose lattice constant does not match the InP substrate [6]. To this end, the contents of In in the $Ga_{1-x}In_xAs$ solid solution is increased, and in the $Al_{1-y}In_yAs$ solid solution it is reduced. As a result, the epitaxial layers are, correspondingly, compressed and stretched with respect to the InP substrate. In such changed compositions of the considered solid solutions, the conduction band offset in the heterojunction noticeably increases; however, it also slightly reduces due to the sign of arising mechanical stresses. Finally, the conduction band offset in such a strain-compensated heteropair increases and at the chosen parameters $x = 0.60$ and $y = 0.42$ we approximately obtain $\Delta E_c = 0.68$ eV. The estimate of the band offset is based on the 'electron affinity' idea [7] for pseudomorphic solid solutions grown on an InP substrate with the compounds specified above. In the estimates, the dependences of the forbidden band gap, lattice constant, deformation values, elastic constants, and deformation potentials on the composition content from [8–10] were used.

The QCL active region comprised of four quantum wells with a 'weakly-diagonal' optical transition was chosen as the working scheme. The calculation was performed for the following active region structure (for a single cascade): **4.0**/1.3/**1.3**/5.1/**1.3**/4.5/**1.4**/4.0/**2.3**/3.1/**1.8**/2.8/**1.9**/2.5/**2.0**/2.4/**2.2**/2.3/**2.8**/2.2, where starting from the injection barrier, the epitaxial layers widths are presented in nanometers. Here, the bold face refers

I.I. Zasavitskii, N.Yu. Kovbasa, N.A. Raspopov P.N. Lebedev Physical Institute, Russian Academy of Sciences, Leninsky prosp. 53, 119991 Moscow, Russia; e-mail: zasavit@sci.lebedev.ru;
A.V. Lobintsov, Yu.V. Kurnyavko, P.V. Gorlachuk OJSC M.F. Stelmakh Polyus Research Institute, ul. Vvedenskogo 3, 117342 Moscow, Russia;
A.B. Krysa, D.G. Revin University of Sheffield, Sheffield, S1 3JD United Kingdom

Received 9 December 2017; revision received 16 January 2018
Kvantovaya Elektronika **48** (5) 472–475 (2018)
Translated by N.A. Raspopov

to the barrier widths, and the quantum well widths are given in ordinary face; the doped layer widths are underlined. The heterostructure design was calculated in order to provide the radiation wavelength of about 5.4 μm.

The electron energy levels and wave functions have been found by solving a one-dimensional Schrödinger equation. The problem stated was solved numerically by the finite-difference method. Since the heterostructure is aimed at room-temperature operation, the chosen calculation parameters corresponded to $T = 300$ K [8, 9]: the conduction band offset is $\Delta E_c = 0.68$ eV, barrier band gap is 1.75 eV, and quantum well gap is 0.68 eV. The electron effective mass in the barrier is $0.11m_0$ and in the well it is $0.05m_0$, where m_0 is the free electron mass. Nonparabolicity of the conduction band was also taken into account.

A calculated energy diagram for the QCL based on a $Ga_{0.4}In_{0.6}As/Al_{0.58}In_{0.42}As$ heteropairis is shown in Fig. 1. One can see that the main transition from upper lasing level 4 to lower lasing level 3 is 'weakly-diagonal', and the energy difference is $E_{43} = 230$ meV, which approximately corresponds to the emission wavelength of 5.4 μm. The energy differences between lower lasing level 3 and level 2 and between levels 2 and 1 are close and approximately equal to 43 meV. Since the injector ground level is below level 1, the obtained voltage defect is above 100 meV. Level 5 is the nearest one to upper level 4, and the distance between them is 58.5 meV, which exceeds the heat energy of $2k_BT$ and gives a hope to obtain the operation temperature of about 300 K.

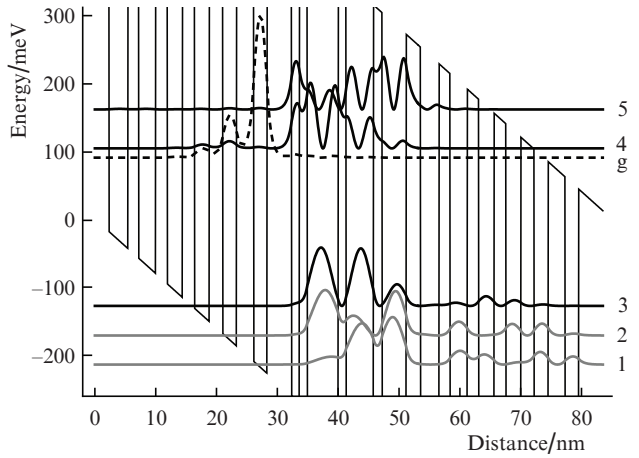

Figure 1. Calculated energy diagram of the active region for the $Ga_{0.4}In_{0.6}As/Al_{0.58}In_{0.42}As$ QCL. The electric field applied is 80 kV cm^{-1}. Square wave function moduli are shown for the important levels.

The laser heterostructure was grown by the MOVPE method on a (001) InP substrate with the electron concentration of 2×10^{18} cm^{-3}. The electron concentration in the doped layers of the active region was 1×10^{17} cm^{-3}. The number of cascades was 35. A thickness of the n-InP waveguide layers was 2.5 μm, and the electron concentration in these layers was 5×10^{16} cm^{-3}.

The X-ray structure was analysed by a DRON-8 diffractometer. A Ω–2θ diffraction scan of the heterostructure studied has a set of well resolved satellites on both sides of the substrate peak (Fig. 2). The zero-order satellite position actually matches that of the substrate. The interference period corresponds to the cascade thickness of 50.5 nm, which is close to the technological value of 51.2 nm. Note that the intensities of the satellite peaks are different on the left and right sides of the zero-order peak. From the model simulation it follows that this intensity ratio corresponds to the indium contents $x = 61.2\%$ in the solid solution $Ga_{1-x}In_xAs$ and $y = 41.9\%$ in $Al_{1-y}In_yAs$, which is close to the technologically prescribed values. Intensities of satellites distant from the zero-order peak are comparatively low and distinct from calculated values. This testifies that the epitaxial layers are smeared to a certain degree (about 0.3–0.7 nm) at each interface, which agrees with data from works utilising other experimental methods for determining roughness of QCL interfaces grown by the MOVPE method [11, 12].

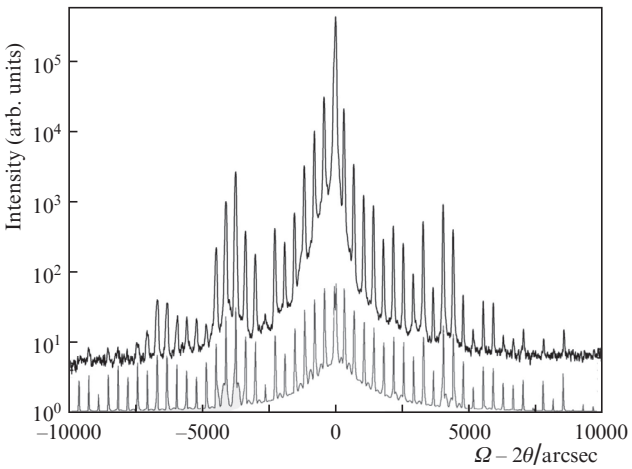

Figure 2. Diffraction Θ–2θ scan of the grown heterostructure (upper curve) and calculated values (lower curve).

Stripes of width 20 μm were formed on the heterostructure by the photolithography technique, and then from the side of layers the plate was totally covered by a dielectric Si_3N_4 layer. Then the dielectric was 'opened' by the photolithography technique in the stripes in order to form ohmic contacts. To this end, the contacts Ti(50 nm)/Au(250 nm) were deposited onto the heterostructure after chemical etching and then it was plated with the Au layer of thickness 2–3 μm. From the side of the substrate, the structure was grounded by chemical-mechanical polishing to a thickness of about 0.15 mm, and Ti/Au contacts were evaporated onto the substrate. Laser crystals chipped with the cavity length of 3 mm were soldered to a copper holder through a thin gasket made of a copper-tungsten alloy for better matching in the coefficients of the linear thermal expansion. Gold conducting leads were welded on the crystal by thermal-compression bonding. The active element produced in this way was mounted on a special holder and placed into a metal optical cryostat with IR-transparent windows made of KBr or BaF_2 or into a compact optical unit comprising a Peltie heatsink for operation at a temperature of down to –20 °C.

3. Measurement results and discussion

Dependences of the threshold current density on temperature were measured in the pulsed regime ($\tau = 1$ μs, $f = 170$ Hz). A gold-doped germanium photoresistor was used as an integral radiation detector. The dependence obtained is presented in Fig. 3. The reached operation temperature of 350 K was lim-

ited by possibilities of the experimental setup. In this case, the threshold current density was at most 1.8 kA cm^{-2}. The threshold current density was 1.6 kA cm^{-2} at 300 K. Thus, the two-phonon depopulation mechanism for the lower lasing level is efficient, and the quantum well is sufficiently deep to reduce electron transition from the upper level to continuum.

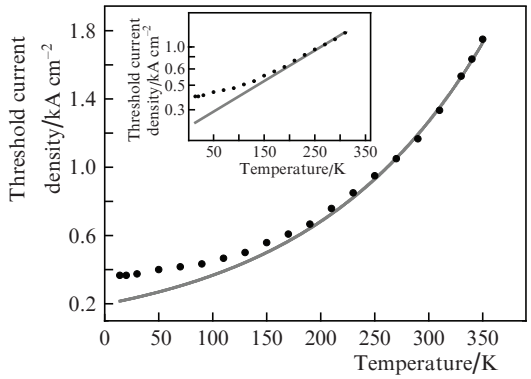

Figure 3. Threshold current density vs. temperature [in the inset: the dependence of $J_{th}(T)$ on the semilogarithmic scale].

A single exponent cannot approximate the temperature dependence of the threshold current density in the whole range of temperature variation 7–350 K. In the range 200–350 K, it can be approximated by the function $J_{th} = 0.2\exp(T/161)$, which is shown in the inset in Fig. 3 on the semilogarithmic scale; thus, the characteristic temperature in this range is $T_0 = (161 \pm 3)$ K.

While measuring power–current characteristics, the laser operated in the pulsed regime as well ($\tau = 50$ ns), but at a pulse repetition rate of 10 kHz. The average radiation power was measured by an OPHIR calorimeter (with the 3A head) at temperatures of 80, 200, and 300 K. Measurement results are shown in Fig. 4. One can see that the laser of size 20 μm× 3 mm with cleaved mirrors has a maximal radiation power of 1.1 W at 80 K and 130 mW at 300 K. This also testifies the efficiency of the active region of the QCL based on a strain-compensated $Ga_{0.4}In_{0.6}As/Al_{0.58}In_{0.42}As$ heteropair.

QCL emission spectra were recorded by a Vertex-70 Fourier spectrometer operated in the step scanning mode with a resolution of 0.2 cm^{-1}. This provided a high resolution

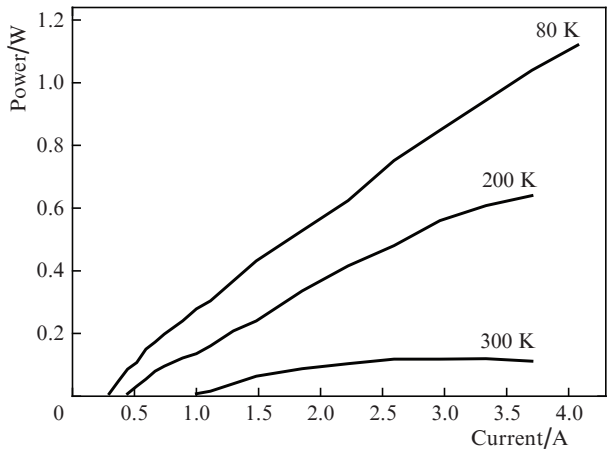

Figure 4. QCL power–current characteristics at various temperatures.

for the mode structure of emission spectra. Results of measurement at two temperatures are given in Fig. 5. At the injection equal to several J_{th}, there are about 100 longitudinal modes in the range 1810–1860 cm^{-1}. The mode separation is 0.505 cm^{-1}. From this value one can find the effective refractive index for the active region $n^* = (2\Delta k L)^{-1} = 3.30$, where Δk is the mode separation and $L = 3$ mm is the cavity length.

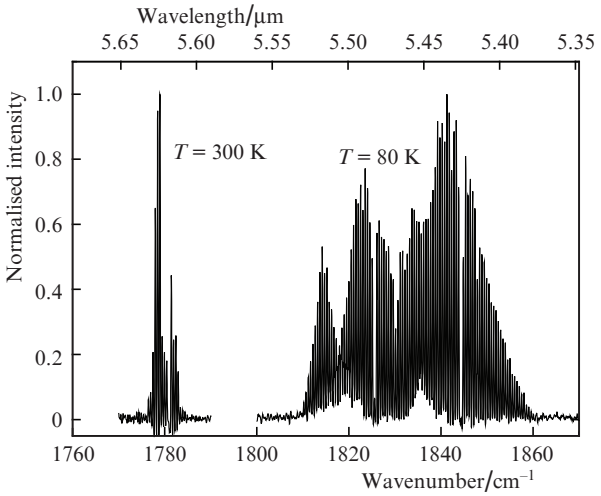

Figure 5. QCL emission spectrum at 80 K and 300 K.

The radiation spectrum profile is affected by active absorption of water vapour because the optical path length of detected emission is ~2 m. By juxtaposing the recorded QCL emission spectrum with known water vapour absorption spectra one can distinguish several bands of various intensity corresponding to water vapour absorption at 1818, 1825, 1830, 1836, and 1844 cm^{-1}. At a higher temperature, the QCL emission spectrum shifts to the long-wavelength side, the spectrum centre shifts from 1835 cm^{-1} at 80 K to 1780 cm^{-1} at 300 K, that is, from 5.45 μm to 5.62 μm. At $T = 300$ K, the spectrum is also affected by absorption of atmospheric water vapour. Note that the emission wavelength of 5.62 μm at room temperature is by 0.2 μm longer than the calculated wavelength (5.4 μm). This is explained by weak smearing of interfaces in the nanoheterostructure, which agrees with data from [11, 12], where interface roughness of the QCLs grown by MOVPE was studied by the transmission electron microscopy. Such a long-wavelength shift was observed in [13] as well, where a QCL was also produced by MOVPE, and the corresponding long-wavelength shift reached as much as 0.5–1 μm.

Thus, a quantum-cascade laser is designed on the basis of a strained-compensated $Ga_{0.4}In_{0.6}As/Al_{0.58}In_{0.42}As$ heteropair, which operates in the wavelength range of 5.5–5.6 μm in the pulsed regime at a temperature of at least 350 K. The QCL has been realised by increasing the quantum well depth and using the two-photon depopulation mechanism for the lower lasing level. The high-quality heterostructure was grown by the MOVPE method. The threshold current density is 1.6 kA cm^{-2} at 300 K. The maximal radiation power of the laser of size 20 μm×3 mm with cleaved mirrors is 1.1 W at 80 K and 130 mW at 300 K.

Acknowledgements. The work was partially (I.I. Zasavitskii, N.Yu. Kovbasa, and N.A. Raspopov) supported by the Presidium of the Russian Academy of Sciences (Programme

I.25P 'Fundamental and applied problems of photonics and physics of new optical materials').

References

1. Faist J., Capasso F., Sirtori C., Sivco D.L., Cho A.Y. *Semiconductors and Semimetals*, **66**, 183 (1999).
2. Faist J. *Quantum Cascade Lasers* (Oxford: University press, 2013).
3. Roberts J.S., Green R.P., Wilson L.R., Zibik E.A., Revin D.G., Cockburn J.W., Airey R.J. *Appl. Phys. Lett*., **82**, 4221 (2003).
4. Green R.P., Krysa A.B., Roberts J.S., Revin D.G., Wilson L.R., Zibik E.A., Ng N.H., Cockburn J.W. *Appl. Phys. Lett*., **83**, 1921 (2003).
5. Krysa A.B., Revin D.G., Commin J.P., Atkins C.N., Kennedy K., Qiu Y., Walther T., Cockburn J.W. *IEEE Photon. Technol. Lett*., **23**, 774 (2011).
6. Faist J., Capasso F., Sivco D.L., Hutchison A.L., Chu S.-N.G., Cho A.Y. *Appl. Phys. Lett*., **72**, 680 (1998).
7. Van de Walle C.G. *Phys. Rev. B*, **39**, 1871 (1989).
8. Vurgaftman I., Meyer J.R., Ram-Mohan L.R. *J. Appl. Phys*., **89**, 5815 (2001).
9. Li E.H. *Physica E*, **5**, 2157 (2000).
10. Kim J., Fischetti M.V. *J. Appl. Phys*., **108**, 013710 (2010).
11. Rajeev A., Chen Weixin, Kirch J.D., Luke J. Mawst L.J., Kuech T.F., Earles T. *Abstracts 21st Am. Conf. on Crystal Growth and Epitaxy/18th US Workshop on Organometallic Vapor Phase Epitaxy* (Santa Fe, NM, USA, 2017) p.275.
12. Walther T., Krysa A.B. *J. Microscopy*, **268**, 298 (2017).
13. Wang C.A., Schwarz B., Siriani D.F., Connors M.K., Missaggia L.J., Calawa D.R., McNulty D., Akey A., Zheng M.C., Donnelly J.P., Mansuripur T.S., Capasso F. *J. Crystal Growth*, **464**, 215 (2017).